1 **Title: Biphasic effect of mechanical stress on lymphocyte activation**

2 **Running title:** Mechanical stress and lymphocyte activation

3 **Authors**

4 Mhd Yousuf Yassouf,[1,2] Xu Zhang,[1,2] Zisheng Huang,[1,2] Da Zhai,[1,2] Reiko Sekiya,[1,2] Tsuyoshi

5 Kawabata,[1,2] Tao-Sheng Li[1,2]*

6 **Affiliations**

7 [1] Department of Stem Cell Biology, Nagasaki University Graduate School of Biomedical Sciences,

8 1-12-4 Sakamoto, Nagasaki 852-8523, Japan.

9 [2] Department of Stem Cell Biology, Nagasaki University Atomic Bomb Disease Institute, 1-12-4

10 Sakamoto, Nagasaki 852-8523, Japan.

11 *Corresponding author. Email: litaoshe@nagasaki-u.ac.jp. Address: Department of Stem Cell

12 Biology, Atomic Bomb Disease Institute, Sakamoto 1-12-4, Nagasaki 852-8523, Japan. Tel: +81-

13 95-819-7097

14 **Conflict of Interest**

15 The authors declare that there is no conflict of interest.

16 **Abstract**

17 Mechanical forces can modulate the immune response, mostly described as promoting the

18 activation of immune cells, but the role and mechanism of pathological levels of mechanical stress

19 in lymphocyte activation have not been focused on before. By ex vivo experimental approach, we

20 observed that mechanical stressing of murine spleen lymphocytes with 50 mmHg for 3 hours

21 induced the nuclear localization of NFAT1, increased C-Jun, and increased the expression of early

22 activation marker CD69 in resting CD8+ cells. Interestingly, 50 mmHg mechanical stressing

23 induced the nuclear localization of NFAT1; but conversely decreased C-Jun and inhibited the

24 expression of CD69 in lymphocytes under LPS (Lipopolysaccharide) or PMA/I (Phorbol 12-

25 myristate 13-acetate/Ionomycin) stimulation. Additionally, we observed similar changes trends

26 when comparing RNA seq data of hypertensive and normotensive COVID-19 patients. Our results

27 indicate a biphasic effect of mechanical stress on lymphocyte activation, which provides insight

28 into the variety of immune responses in pathologies involving elevated mechanical stress.

29

Introduction

Mechanical forces play an essential role in maintaining the homeostasis of our body. Various mechanical forces, such as shear stress and hydrostatic pressure are known to regulate the biological properties of cells, especially in the circulatory and immunological systems. In the past decade, mechanosensing and mechanotransduction of cells in response to different mechanical forces have been one of the hottest topics of life science. However, the precise role and relevant molecular mechanism of mechanical forces in the biological properties of tissue cells is still poorly understood because it is extremely difficult to distinct the mechanical forces from other factors by in vivo experimental approach.

Previous studies have explored the mechanical stress-induced responses of different cell types using various mechanical cues, including stretch stress (Coste et al., 2010), shear stress (Ranade et al., 2014), hydrostatic pressure (Solis et al., 2019), and various degrees of scaffold stiffness (Atcha et al., 2021). Among numerous mechanotransduction key molecules, PIEZO1, a mechanosensitive ion channel, has been focused on recently due to its multiple functions and wide expression in all organs. PIEZO1 has been demonstrated to be essential in cyclical hydrostatic pressure sensing for the proper response of macrophages in case of lung infection (Solis et al., 2019).

The role of mechanical forces and stiffness has been reported in triggering the activation of lymphocytes (Judokusumo et al., 2012; Li et al., 2010; Ma & Finkel, 2010), macrophages (Solis et al., 2019), and myeloid cells (Aykut et al., 2020), suggesting that mechanical cues may promote the activation of immune cells. On the other hand, under pathological conditions, mechanical forces around the tissue cells can be altered dynamically, such as the increased mechanical stress in patients with hypertension. Therefore, it will be possible that elevated hydrostatic pressure

55 induces the activation of circulating leukocytes but may conversely impair their activation and

56 function in response to severe infections, as clinical studies indicated worse outcomes and severity

57 for hypertensive patients who suffer serious infections (Guan et al., 2020; Piroth et al., 2021;

58 Schoen et al., 2019). Thus, we were interested to investigate the precise role and molecular

59 mechanism of elevated mechanical stress, specifically elevated pathological levels of hydrostatic

60 pressure, in lymphocyte activation as it has not been focused on previously.

61 **Materials and Methods**

62 **Animals and cell culture**

63 C57BL/6 male mice (CLEA, Tokyo, Japan), 8 to 12 weeks old, were used in this study for spleen

64 harvest. The animals were bred in specific, pathogen-free conditions and were allowed free access

65 to food and water in a temperature-controlled environment with a 12:12-h light–dark cycle. All

66 animal procedures were performed in accordance with institutional and national guidelines.

67 Freshly harvested spleens were cut using surgical blade then strained against 70 μm cell strainer

68 using gentle pressure applied by syringe plug while adding phosphate-buffered saline (PBS).

69 Suspended spleen cells were collected, and then red blood cells were lysed using RBC lysis

70 (Invitrogen, Waltham, Massachusetts, USA) according to manufacturer's instructions. Resulting

71 cells were strained against 40 μm cell strainer to discard any cell aggregates, then suspended at a

72 density of 5×10^6 cells/mL in RPMI-1640 with L-glutamine (Wako, Osaka, Japan) supplemented

73 with 10% fetal bovine serum (HyClone FBS, GE Healthcare, Chicago, Illinois, USA), 100 U/mL

74 penicillin and 100 μg/mL streptomycin (Wako, Japan), and 50 μM 2-mercaptoethanol (Sigma,

75 Burlington, MA, USA) at 37°C in a 5% CO2-humified atmosphere, all following treatments were

76 applied after 3 hours of cells incubation. In some experiments, lymphocytes were treated with

77 Piezo1 agonist Yoda1 at 10 μM concentration (Cayman Chemical, Michigan, USA), ROCK

4

78   inhibitor Y27632 at 10 μM concentration (ATCC, Manassas, Virginia, USA), and O55:B5 E. coli

79   Lipopolysaccharides at 1 μg/mL concentration (LPS, Sigma, USA). Cell activation cocktail

80   (Phorbol 12-myristate 13-acetate/Ionomycin) was purchased from Bio-Legend (San Diego,

81   California, USA) and used at the concentrations suggested by manufacturer (PMA/I: PMA 81 nM,

82   ionomycin 1.34 μM) (Reagents are described in Table S1).

83   **Mechanical stress**

84   For mechanical stress, culture dishes were subjected to static pressure using a hydrostatic pressure

85   system from STREX (STREX AGP-3001S, Osaka, Japan) which was placed inside a 5% CO_2 cell

86   culture incubator at 37°C (Figure S1). The compressor unit intakes the air from the 5% CO_2

87   balanced air within the cell culture incubator, then injects into the sealed chamber. The compressor

88   unit has a sensitive sensor to measure the pressure inside the chamber and adjust it to the value

89   assigned using the controllers on the compressor unit. We used 50 mmHg for the purpose of this

90   experiment.

91   **Flow cytometry**

92   Following incubation in the various culture conditions, cells were harvested and directly washed

93   with cold PBS for 5 min at 1400×g at 4°C, then 5×10^5 cells from each condition were re-suspended

94   in FACS buffer (4% FBS, cold PBS) and incubated with Fc block for 15 min, followed by adding

95   conjugated antibodies for CD4, CD8, CD19, and CD69 to each tube and incubated for 30 min at

96   4°C (dilutions and conjugated fluorochromes are described in Table S2). After staining and

97   washing, cells were suspended in FACS buffer and data was acquired on BD FACSVerse (BD

98   Biosciences, Franklin Lakes, New Jersey, USA). A minimum of 10,000 cell counts were analyzed.

99   **RNA isolation and RTqPCR**

100   Following incubation in the various culture conditions, cells were harvested and directly washed

101   with cold PBS for 5 min at 1400×g at 4°C, then resulting cell pellets were used to isolate total

102   RNA (approximately 10^7 cells in each pellet) using Quick-RNA™ Microprep Kit (Zymo Research,

103   Irvine, California, USA) according to manufacturer's instructions. RNA quantity and quality were

104   assessed using NanoDrop™ 2000/2000c (Thermo Fisher Scientific, Waltham, Massachusetts,

105   USA). cDNA was generated using 900 ng of purified total RNA with SuperScript™ VILO™

106   MasterMix (Invitrogen, USA) according to manufacturer's instructions. The amplified cDNA was

107   diluted at a ratio of 1:10 in DNase- and RNase- free water. RTqPCR reactions were performed

108   using 2 µL cDNA (equivalent to 18 ng total RNA) per reaction with THUNDERBIRD SYBR

109   qPCR Mix (TOYOBO, Osaka, Japan) on LightCycler® 480 Instrument II (Roche Life Science,

110   Basel, Switzerland) according to manufacturer's instructions. Fold changes of expression are

111   relative to the control using $2^{-\Delta C'T}$ method (Livak & Schmittgen, 2001). Primers sequences are

112   listed in Table S3.

113   **ELISA**

114   The levels of IL-2, IFN-γ, and TNF-a in supernatants were determined by sandwich ELISA using

115   LEGEND MAX™ Mouse IL-2 ELISA Kit, LEGEND MAX™ Mouse IFN-γ ELISA Kit, and

116   LEGEND MAX™ Mouse TNF-a ELISA Kit, respectively (BioLegend, USA) according to

117   manufacturer's instructions. Optical densities were acquired using iMark Microplate Reader (Bio-

118   Rad, USA).

119   **Immunocytochemistry**

120   Following incubation in the various culture conditions, stimulations were stopped by addition of

121   10 volumes of ice-cold PBS then cells were pelleted at 1400×g at 4°C, and $5×10^5$ cells from each

122   condition were re-suspended in FACS buffer (4% FBS, cold PBS) and incubated with Fc block

for 15 min, followed by adding conjugated antibodies for CD4, and CD8 to each tube and incubated for 60 min in dark at 4°C (dilutions and conjugated fluorochromes are described in Table S2). After staining, cells were washed twice and suspended in fixation/permeabilization buffer (Invitrogen) for 60 min in dark at 4°C, then washed with permeabilization buffer (Invitrogen) two times 5 min each, at 1400×g at 4°C, then blocked in 3% BSA for 20 min, followed by 60 min incubation in dark with primary antibodies against NFAT1 (Cell Signaling Technology, Danvers, Massachusetts, USA) or HIF1-α (Novus Biologicals, Centennial, Colorado, USA). Cells were washed and incubated with Alexa Fluor 546- or Alexa Fluor 647-conjugeted secondary antibodies for 60 min in dark. After washing, cells were incubated with DAPI (4′,6-diamidino-2-phenylindole, Invitrogen) for 30 min in dark. Stained cells were attached to microscope slides by centrifugation for 3 min at 112.9 g using Cytospin 3 (Thermo Shandon, USA) followed by adding Vectashield Vibrance mounting medium (Vector laboratories, Burlingame, California, USA) and coverslips. The cells were viewed using 63x oil-immersion objective lens on LSM 800 confocal microscope (Zeiss, Oberkochen, Germany). Fluorescent image analysis for quantification and localization estimates were performed with the NIH ImageJ software package using the same image analysis workflow for all images in all replicates.

RNA sequencing dataset analysis

The RNA sequencing raw data were downloaded from the gene expression omnibus (GEO) database (Barrett et al., 2013) with accession number GSE157859 (Zheng et al., 2020). GSE157859 included RNA sequencing data prepared from peripheral venous blood samples of patients with COVID-19 which were obtained at different clinical stages. Among those patients, 4 patients have hypertension as the only main comorbidity (Hypertensive patients: HT), and we selected 4 closest matching patients with no comorbidities as control group (Normotensive

patients: NT), we compared the data from 4 HT patients (GSM4776962, GSM4776976, GSM4776981, GSM4776985) with 4 NT patients (GSM4776954, GSM4776964, GSM4776967, GSM4776974) in the treatment clinical stage, also in the rehabilitation stage 2 HT patients (GSM4776978, GSM4776987) with 3 NT patients (GSM4776956, GSM4776966, GSM4776969) data were available for comparison. The raw sequencing data were uploaded to the Galaxy web platform, and we used the public server at usegalaxy.org to analyze the data (Afgan et al., 2016). Quality of data were checked by FastQC v0.11.8 (Andrews, 2010) followed by Adapters removal, reads trimming, and quality filtering using Fastp v0.20.1 (Chen et al., 2018). The clean reads were then aligned to the primary assembly of the human reference genome, GRCh38, using HISAT2 v2.1.0 (Kim et al., 2015). We used featureCounts v2.0.1 (Liao et al., 2014) to count RNA-seq reads for genes with GRCh38 annotation. Finally, edgeR v3.24.1 (Robinson et al., 2010) was used to perform differential expression testing and estimating log2 fold change [HT-NT].

Statistical analysis

All results are presented as the means ± SD. Statistical significance between two groups was determined using t-test. Differences were considered significant when two-sided $p<0.05$.

Results

Mechanical stress enhances CD69 expression in resting CD8+ cells, but conversely impairs the activation of lymphocytes under LPS or PMA/I stimulation

Lymphocytes were collected from the mouse spleen and then incubated without (Resting) or with the addition of LPS or PMA/I in medium (Stimulated). To investigate the potential effect of mechanical stress on lymphocyte activation, we used a bioreactor capable of subjecting cells to 50 mmHg pressure for 3 hours, and as a control, cells were placed in the atmospheric pressure, both

169   inside a 5% CO_2 incubator at 37°C (Figure S1). We evaluated the expression of the early activation

170   marker CD69 using flow cytometry. In resting lymphocytes, mechanical stress significantly

171   increased the expression of CD69 in CD8+ T cells (31.8 ± 3.2 versus 22.78 ± 1.95, $p < 0.01$; Figure

172   1. A). However, with the addition of LPS in the medium, mechanical stress significantly decreased

173   the expression of CD69 in CD19+ B cells (2841 ± 1178 versus 5177 ± 1570, $p < 0.01$; Figure 1.

174   A). Similarly, under the stimulation with PMA/I, mechanical stress significantly decreased the

175   expression of CD69 in CD4+ T cells (9188 ± 855.5 versus 18461 ± 1455, $p < 0.01$; Figure 1. A),

176   CD8+ T cells (9314 ± 753.5 versus 22499 ± 1453, $p < 0.01$; Figure 1. A), and CD19+ B cells

177   (13642 ± 3789 versus 16227 ± 3497, $p = 0.02$; Figure 1. A). CD19+ B cells respond to LPS

178   stimulation because of the TLR4 receptor on murine B cells recognizing LPS. On the other hand,

179   murine CD4+ and CD8+ T cells do not respond to LPS due to the absence of the TLR4 receptor

180   (Applequist et al., 2002).

181   We also evaluated the mRNA expression of several major cytokines using RT-qPCR. In resting

182   lymphocytes, mechanical stress significantly decreased the mRNA level of *Il2* ($p < 0.01$; Figure 1.

183   B), but increased the mRNA level of *Ifng* ($p = 0.06$; Figure 1. B). Interestingly, with the addition

184   of LPS in medium, mechanical stress significantly decreased the mRNA levels of *Il1b* ($p = 0.01$;

185   Figure 1. B), *Il2* ($p = 0.09$; Figure 1. B) and *Il10* ($p = 0.02$; Figure 1. B). Similarly, under PMA/I

186   stimulation, mechanical stress significantly decreased the mRNA levels of *Ifng* ($p < 0.01$; Figure 1.

187   B), *Il2* ($p = 0.01$; Figure 1. B), *Il4* ($p = 0.03$; Figure 1. B), and *Il10* ($p < 0.01$; Figure 1. B), while

188   increased the mRNA level of *Tnf* ($p = 0.02$; Figure 1. B).

189   To further confirm our findings, we measured the protein levels of IFN-γ, IL-2, and TNF-a in the

190   culture medium using ELISA. In resting lymphocytes, mechanical stress only slightly increased

191   the secretion of IFN-γ ($p = 0.056$; Figure 1. C). However, for PMA/I-stimulated lymphocytes,

192 mechanical stress significantly decreased the secretion of IFN-γ ($p< 0.01$; Figure 1. C), IL-2 ($p<$

193 0.01; Figure 1. C), and TNF-a ($p= 0.01$; Figure 1. C).

194 IL-2 is usually secreted from activated CD4+ and CD8+ T cells. According to our data, mechanical

195 stress decreased the mRNA expression of *Il2* in both resting and PMA/I-stimulated lymphocytes

196 but induced CD69 expression in resting CD8+ cells. We speculated that the expression change in

197 IL-2 might be related to the effect of mechanical stress on CD4+ T cells. Therefore, mechanical

198 stress may promote the activation of resting CD8+ T cells, but likely shows an inhibitory effect on

199 lymphocyte activation under the stimulation with PMA/I or LPS.

200 **RhoA/ROCK pathway and PIEZO1 are not closely involved in the mechanical stress-**

201 **induced inhibition on the activation of PMA/I-stimulated lymphocytes**

202 Previous studies have described that cellular response to mechanical forces is regulated through

203 RhoA/ROCK pathway (Boyle et al., 2020; Takemoto et al., 2015; Teramura et al., 2012), and

204 ROCK inhibition has been demonstrated to suppress lymphocyte activation (Aihara et al., 2003;

205 Lou et al., 2001; Tharaux et al., 2003). Therefore, we investigated whether mechanical stress

206 inhibited lymphocyte activation through RhoA/ROCK pathway. We incubated lymphocytes with

207 or without Y27632, a ROCK inhibitor, at 10 μM as previous studies suggest this concentration to

208 show its maximum effects (Aihara et al., 2003; Bardi et al., 2003). Unexpectedly, ROCK inhibition

209 did not obviously mitigate the mechanical stress-induced changes in the expression of CD69 in

210 PMA/I-stimulated lymphocytes (Figure S2. A), as well as their secretion of IFN-γ, IL-2, and TNF-

211 a. Instead, ROCK inhibition even enhanced the inhibition in some of these parameters (Figure S2.

212 B). Therefore, the RhoA/ROCK pathway might not be closely involved in the mechanical stress-

213 induced inhibition of lymphocyte activation under PMA/I stimulation.

214 Studies have also focused on the role of PIEZO1 in the function and activation of myeloid cells

215 (Aykut et al., 2020), macrophages (Solis et al., 2019), T lymphocytes (Liu et al., 2018). BioGPS

216 gene portal data also showed that murine T lymphocytes express considerable amounts of PIEZO1

217 similar to macrophages (Figure S3) (Lattin et al., 2008; Wu et al., 2009). Thus, we investigated

218 whether PIEZO1 is involved in the observed effects of mechanical stress on lymphocyte activation.

219 We incubated resting and PMA/I-stimulated lymphocytes with or without Yoda1, a PIEZO1

220 agonist, for 3 hours followed by evaluations. For resting lymphocytes, Yoda1 significantly

221 increased the expression of CD69 in CD8+ T cells ($p < 0.01$; Figure 2. A). For PMA/I-stimulated

222 lymphocytes, Yoda1 conversely decreased CD69 expression in CD4+ T cells ($p < 0.01$; Figure 2.

223 A) and CD8+ T cells ($p < 0.01$; Figure 2. A), but did not significantly change CD69 expression in

224 CD19+ B cells (Figure 2. A).

225 ELISA testing of culture medium showed that Yoda1 slightly induced the secretion of IFN-γ from

226 resting lymphocytes ($p = 0.02$; Figure 2. B). Differed from mechanical stress, Yoda1 did not

227 change the secretion of IL-2 but increased the secretion of IFN-γ ($p = <0.01$; Figure 2. A) and TNF-

228 a ($p = 0.03$; Figure 2. B) from PMA/I-stimulated lymphocytes. PIEZO1 agonist and mechanical

229 stress significantly and very similarly promoted CD69 expression in resting CD8+ cells and

230 inhibited CD69 expression in PMA/I-stimulated lymphocytes, however, they intriguingly showed

231 opposite effects on cytokine secretion. This suggests that mechanisms other than PIEZO1

232 mechanosensing by which mechanical stress inhibits the secretion of cytokines from PMA/I-

233 stimulated lymphocytes.

234 **Mechanical stress promotes nuclear HIF1-α localization in resting but not PMA/I-stimulated**

235 **lymphocytes**

It has been reported that mechanical loading induces HIF1-α expression and nuclear localization (Jing et al., 2020). Several previous studies have also reported an increased expression of HIF1-α in activated T lymphocytes (Nicoli et al., 2018; Wang et al., 2011) and mast cells (Walczak-Drzewiecka et al., 2008). As the enhanced activity of HIF1-α may promote the effector function of CD8+ T cells (Palazon et al., 2014), we measured HIF1-α expression and localization. We incubated resting and PMA/I-stimulated murine spleen lymphocytes with or without 50 mmHg mechanical stressing for 3 hours. In resting lymphocytes, mechanical stress induced the nuclear localization of HIF1-α in both CD4+ and CD8+ T cells (Figure S4). PMA/I-stimulated lymphocytes expressed higher HIF1-α compared to resting ones. In PMA/I-stimulated lymphocytes, there was no significant difference between mechanically stressed or not, although PMA/I-stimulated CD8+ lymphocytes tend to have decreased nuclear HIF1-α under mechanical stress (Figure S4). Mechanical stress did not change the mRNA levels of *Hif1a* in resting lymphocytes but showed to inhibit the enhancement of *Hif1a* expression in PMA/I-stimulated lymphocytes ($p= 0.095$; Figure S5). Based on our results, mechanical stress induced HIF1-α nuclear localization in resting lymphocytes, but conversely inhibited the enhancement of *Hif1a* mRNA expression in PMA/I-stimulated lymphocytes, supporting the inhibitory effect of mechanical stress in PMA/I-stimulated lymphocytes.

Mechanical stress induces NFAT1 nuclear localization but reduces Jun expression in PMA/I-stimulated lymphocytes

It is well known that increased mechanical stress can increase intracellular Ca^{2+} levels (Hamill & Martinac, 2001). Increased calcium levels within the cytoplasm of T lymphocytes lead to the dephosphorylation of NFAT followed by its nuclear localization to initiate the transcription program (McCaffrey et al., 1993; Northrop et al., 1994). Thus, we tried to investigate whether

259   NFAT1 is involved in the inhibitory effect of mechanical stress on the activation of PMA/I-

260   stimulated lymphocytes. In resting lymphocytes, mechanical stress exactly increased the nuclear

261   levels of NFAT1 in both CD4+ and CD8+ cells (Figure 3). Similarly, for PMA/I-stimulated

262   lymphocytes, mechanical stress also induced the nuclear localization of NFAT1 in both CD4+ and

263   CD8+ cells (Figure 3).

264   NFAT1 nuclear localization might initiate either T lymphocyte activation or anergy, depending on

265   the availability of other transcription factors such as AP1 (Hogan, 2017; Macián et al., 2002).

266   Cooperation of NFAT with AP-1 (C-Jun: C-Fos) is essential for proper activation of lymphocytes,

267   thus we further investigated the expression of AP-1. In resting lymphocytes, mechanical stress

268   significantly increased the mRNA level of *Jun* (p= 0.02; Figure 4). Conversely, under PMA/I

269   stimulation, mechanical stress significantly decreased mRNA levels of *Jun* (p= 0.04; Figure 4).

270   While mechanical stress did not alter *Fos* mRNA levels in either resting or PMA/I-stimulated

271   lymphocytes. As mechanical stress showed to promote NFAT1 nuclear localization but to decrease

272   *Jun* expression in PMA/I-stimulated lymphocytes, mechanical stress may suppress *Jun* to impair

273   the activation of PMA/I-stimulated lymphocytes.

274   **Hypertensive COVID19 patients have altered *JUN* and *CD69* expression**

275   Hypertension imposes circulating leukocytes to elevated hydrostatic pressure. Clinical studies

276   have reported the worse outcome of infections in patients with hypertension than that of without

277   (Guan et al., 2020; Piroth et al., 2021; Schoen et al., 2019). Out of 165 hypertensive COVID-19

278   patients, 41 (24.85%) patients have developed severe symptoms, while of the 495 COVID-19

279   patients without comorbidities, only 10 (2.02%) patients were severe cases (Guan et al., 2020).

280   Another study has found that out of the patients hospitalized for COVID-19 and seasonal influenza,

281   33.1% and 28.2% of cases, respectively, have the comorbidity of hypertension (Piroth et al., 2021).

282 Additionally, it has been found that the presence of hypertension on hospital admission was

283 associated with worse clinical outcomes in patients with H1N1 influenza A virus infection (Schoen

284 et al., 2019). Therefore, we were interested in searching whether lymphocyte activation-related

285 genes are associated with the development of severe symptoms in hypertensive COVID19 patients.

286 We analyzed RNA sequencing data prepared from PBMC of COVID19 patients with hypertension

287 or without. PBMCs were collected at the treatment stage (15.9 ± 8.1 days after infection day) and

288 rehabilitation stage (67.2 ± 6.4 days after infection day), probably similar to the stimulated

289 lymphocytes and resting lymphocytes, respectively (Zheng et al., 2020). Results show that, in the

290 treatment stage, hypertensive COVID19 patients [HT] have reduced *JUN* and *CD69* expression

291 compared to normotensive COVID19 patients [NT] (Figure 5). Conversely, in the rehabilitation

292 stage, hypertensive patients have higher *JUN*, *FOS*, *CD69*, and *TNF* expression compared to

293 normotensive ones (Figure 5). These results suggest the likely relationship between *JUN*

294 expression and lymphocyte activation changes in hypertensive patients. Therefore, we speculate

295 that hypertensive patients may have impaired immune response to serious infections, like the

296 COVID19.

Discussion

298 In this study, we investigated the effect of elevated mechanical stress in lymphocyte activation by

299 ex vivo experimental approach. We mechanically stressed murine spleen lymphocytes with 50

300 mmHg either in the resting state (no-stimulation) or in LPS- or PMA/I-stimulated state. Our data

301 indicated that mechanical stress induced CD69 expression of resting CD8+ cells but conversely

302 impaired lymphocyte activation under the LPS or PMA/I stimulation. Based on our ex vivo

303 experimental data, it seems that mechanical stress can induce the activation of resting lymphocytes

304 but may conversely impair lymphocyte activation when responding to exogenous stimulations or

305 severe infections.

306 In searching for mechanotransduction key molecule(s) involved in the observed biphasic effects

307 of mechanical stress on lymphocyte activation, we found that RhoA/ROCK pathway might not be

308 closely involved in the mechanical stress-induced inhibition of lymphocyte activation under

309 PMA/I stimulation. Liu et al showed that Yoda1, PIEZO1 agonist, rescued the activation and CD69

310 expression of CD4+ and CD8+ T cells treated with soluble anti-CD3/anti-CD28 Abs, however in

311 that study, the single effect of Yoda1 treatment was not explained, nor the effect of Yoda1 addition

312 to properly activated T cells (Liu et al., 2018). While, in this study, we showed a similar effect of

313 Yoda1 and mechanical stress on CD69 expression, where both promote its expression in resting

314 CD8+ cells and reduce it in PMA/I-stimulated lymphocytes. However, cytokines expression

315 profiles of PMA/I-stimulated lymphocytes were interestingly different between PIEZO1 agonist

316 Yoda1 and mechanical stress. PIEZO1 agonist promoted IFN-γ and TNF-a secretion which agrees

317 with the enhanced inflammatory activation by Yoda1 in IFN-γ/LPS stimulated macrophages

318 (Atcha et al., 2021), but mechanical stress conversely inhibited their secretion along with IL-2,

319 suggesting that mechanisms other than PIEZO1 mechanosensing by which mechanical stress

320 inhibits the expression of cytokines in PMA/I-stimulated lymphocytes. Additionally, we found

321 that mechanical stress may alter HIF1-α nuclear localization and levels in a trend going along with

322 the biphasic effect of mechanical stress in lymphocyte activation.

323 Mechanical stress may increase intracellular Ca^{2+} levels [20], and the increased cytoplasm Ca^{2+}

324 levels in T-lymphocytes can lead to NFAT nuclear localization [21, 22]. We found that mechanical

325 stress promoted NFAT1 nuclear localization in both resting and PMA/I-stimulated lymphocytes.

326 On the other hand, mechanical stress increased Jun expression in resting lymphocytes but

327 decreased Jun expression in PMA/I-stimulated lymphocytes. As C-Jun cooperation with NFAT is

328 known to be essential for the proper activation of T-lymphocytes (Hogan, 2017; Macián et al.,

329 2002), the alteration of *Jun* expression may provide a reasonable explanation of the different

330 effects of mechanical stress on lymphocyte activation, as observed in our study. With the

331 mechanical stress, enhanced *Jun* may induce the activation in resting CD8+ lymphocytes, while

332 the imbalance between NFAT1 and *Jun* can suppress the activation of lymphocytes in response to

333 PMA/I stimulation.

334 Considering the clinical relevance of our finding from ex vivo experiments, especially at the lasting

335 pandemic situation of COVID19, we analyzed RNAseq data from both hypertensive and

336 normotensive COVID19 patients. At the treatment stage, hypertensive COVID19 patients have

337 reduced *JUN* and *CD69* expression compared to normotensive ones, and the opposite at the

338 rehabilitation stage. Interestingly, C-Jun which is an important transcription factor to promote the

339 activation program of lymphocytes mediated by NFAT1 nuclear localization is reduced in

340 hypertensive COVID19 patients at the treatment stage and conversely increased at the

341 rehabilitation stage. This observation directed us to evaluate C-Jun and C-Fos expression in our

342 experimental setup where we surprisingly found the same trend of *Jun* changes in mechanically

343 stressed murine lymphocytes. *Jun* was described as one of the immediate-early genes in response

344 to mechanical stress in cardiac myocytes (Komuro & Yazaki, 1993; Sadoshima & Izumo, 1997),

345 but for lymphocytes, our study is the first report for the different effect of mechanical stress on

346 *Jun* expression between resting and PMA/I-stimulated lymphocytes.

347 Biphasic response of T cells spreading-behavior to substrate stiffness has been described (Wahl et

348 al., 2019), where high stiffness lead to either increased or decreased T cell spreading depending

349 on whether the substrate is functionalized with both anti-CD3 and ICAM-1 or with anti-CD3 only,

350 respectively. The biphasic response of T cells spreading-behavior to substrate stiffness may

351 indirectly support the observed biphasic response of lymphocytes to mechanical stress in our study,

352 as T cell spreading is important for their activation.

353 Our experimental results provide direct evidence about the biphasic effect of mechanical stress in

354 lymphocyte activation. As mechanical stress will be commonly elevated in various pathological

355 conditions, finding from this study provides novel mechanistic insight into the increased risk of

356 serious infection in individuals with comorbidities involving increased mechanical stress, such as

357 hypertension and diabetes mellitus.

358

375 **Conflict of Interest**

376 The authors declare that there is no conflict of interest.

377 **Data Availability**

378 The data that support the findings of this study are available from the corresponding author upon

379 reasonable request.

380 **References**

381 Afgan, E., Baker, D., van den Beek, M., Blankenberg, D., Bouvier, D., Čech, M., . . . Goecks, J.
382 (2016). The Galaxy platform for accessible, reproducible and collaborative biomedical
383 analyses: 2016 update. *Nucleic Acids Res, 44*(W1), W3-w10. doi:10.1093/nar/gkw343
384 Aihara, M., Dobashi, K., Iizuka, K., Nakazawa, T., & Mori, M. (2003). Comparison of effects of
385 Y-27632 and Isoproterenol on release of cytokines from human peripheral T cells. *Int*
386 *Immunopharmacol, 3*(12), 1619-1625. doi:10.1016/s1567-5769(03)00184-x
387 Andrews, S. (2010). FASTQC. A quality control tool for high throughput sequence data. In.
388 Applequist, S. E., Wallin, R. P., & Ljunggren, H. G. (2002). Variable expression of Toll-like
389 receptor in murine innate and adaptive immune cell lines. *Int Immunol, 14*(9), 1065-1074.
390 doi:10.1093/intimm/dxf069
391 Atcha, H., Jairaman, A., Holt, J. R., Meli, V. S., Nagalla, R. R., Veerasubramanian, P. K., . . .
392 Liu, W. F. (2021). Mechanically activated ion channel Piezo1 modulates macrophage
393 polarization and stiffness sensing. *Nature Communications, 12*(1), 3256.
394 doi:10.1038/s41467-021-23482-5
395 Aykut, B., Chen, R., Kim, J. I., Wu, D., Shadaloey, S. A. A., Abengozar, R., . . . Miller, G.
396 (2020). Targeting Piezo1 unleashes innate immunity against cancer and infectious
397 disease. *Sci Immunol, 5*(50). doi:10.1126/sciimmunol.abb5168
398 Bardi, G., Niggli, V., & Loetscher, P. (2003). Rho kinase is required for CCR7-mediated
399 polarization and chemotaxis of T lymphocytes. *FEBS Lett, 542*(1-3), 79-83.
400 doi:10.1016/s0014-5793(03)00351-x
401 Barrett, T., Wilhite, S. E., Ledoux, P., Evangelista, C., Kim, I. F., Tomashevsky, M., . . .
402 Soboleva, A. (2013). NCBI GEO: archive for functional genomics data sets--update.
403 *Nucleic Acids Res, 41*(Database issue), D991-995. doi:10.1093/nar/gks1193
404 Boyle, S. T., Kular, J., Nobis, M., Ruszkiewicz, A., Timpson, P., & Samuel, M. S. (2020). Acute
405 compressive stress activates RHO/ROCK-mediated cellular processes. *Small GTPases,*
406 *11*(5), 354-370. doi:10.1080/21541248.2017.1413496
407 Chen, S., Zhou, Y., Chen, Y., & Gu, J. (2018). fastp: an ultra-fast all-in-one FASTQ
408 preprocessor. *Bioinformatics, 34*(17), i884-i890. doi:10.1093/bioinformatics/bty560

409   Coste, B., Mathur, J., Schmidt, M., Earley, T. J., Ranade, S., Petrus, M. J., . . . Patapoutian, A.
410   (2010). Piezo1 and Piezo2 Are Essential Components of Distinct Mechanically Activated
411   Cation Channels. *330*(6000), 55-60. doi:doi:10.1126/science.1193270

412   Guan, W.-j., Ni, Z.-y., Hu, Y., Liang, W.-h., Ou, C.-q., He, J.-x., . . . Zhong, N.-s. (2020).
413   Clinical Characteristics of Coronavirus Disease 2019 in China. *N Engl J Med, 382*(18),
414   1708-1720. doi:10.1056/NEJMoa2002032

415   Hamill, O. P., & Martinac, B. (2001). Molecular basis of mechanotransduction in living cells.
416   *Physiol Rev, 81*(2), 685-740. doi:10.1152/physrev.2001.81.2.685

417   Hogan, P. G. (2017). Calcium-NFAT transcriptional signalling in T cell activation and T cell
418   exhaustion. *Cell calcium, 63*, 66-69. doi:10.1016/j.ceca.2017.01.014

419   Jing, X., Yang, X., Zhang, W., Wang, S., Cui, X., Du, T., & Li, T. (2020). Mechanical loading
420   induces HIF-1α expression in chondrocytes via YAP. *Biotechnol Lett, 42*(9), 1645-1654.
421   doi:10.1007/s10529-020-02910-4

422   Judokusumo, E., Tabdanov, E., Kumari, S., Dustin, M. L., & Kam, L. C. (2012).
423   Mechanosensing in T lymphocyte activation. *Biophysical journal, 102*(2), L5-L7.
424   doi:10.1016/j.bpj.2011.12.011

425   Kim, D., Langmead, B., & Salzberg, S. L. (2015). HISAT: a fast spliced aligner with low
426   memory requirements. *Nat Methods, 12*(4), 357-360. doi:10.1038/nmeth.3317

427   Komuro, I., & Yazaki, Y. (1993). Control of cardiac gene expression by mechanical stress. *Annu*
428   *Rev Physiol, 55*, 55-75. doi:10.1146/annurev.ph.55.030193.000415

429   Lattin, J. E., Schroder, K., Su, A. I., Walker, J. R., Zhang, J., Wiltshire, T., . . . Sweet, M. J.
430   (2008). Expression analysis of G Protein-Coupled Receptors in mouse macrophages.
431   *Immunome Res, 4*, 5. doi:10.1186/1745-7580-4-5

432   Li, Y.-C., Chen, B.-M., Wu, P.-C., Cheng, T.-L., Kao, L.-S., Tao, M.-H., . . . Roffler, S. R.
433   (2010). Cutting Edge: Mechanical Forces Acting on T Cells Immobilized via the TCR
434   Complex Can Trigger TCR Signaling. *J Immunol, 184*(11), 5959.
435   doi:10.4049/jimmunol.0900775

436   Liao, Y., Smyth, G. K., & Shi, W. (2014). featureCounts: an efficient general purpose program
437   for assigning sequence reads to genomic features. *Bioinformatics, 30*(7), 923-930.
438   doi:10.1093/bioinformatics/btt656

439   Liu, C. S. C., Raychaudhuri, D., Paul, B., Chakrabarty, Y., Ghosh, A. R., Rahaman, O., . . .
440   Ganguly, D. (2018). Cutting Edge: Piezo1 Mechanosensors Optimize Human T Cell
441   Activation. *J Immunol, 200*(4), 1255-1260. doi:10.4049/jimmunol.1701118

442   Livak, K. J., & Schmittgen, T. D. (2001). Analysis of Relative Gene Expression Data Using
443   Real-Time Quantitative PCR and the 2−ΔΔCT Method. *Methods, 25*(4), 402-408.
444   doi:10.1006/meth.2001.1262

445   Lou, Z., Billadeau, D. D., Savoy, D. N., Schoon, R. A., & Leibson, P. J. (2001). A role for a
446   RhoA/ROCK/LIM-kinase pathway in the regulation of cytotoxic lymphocytes. *J*
447   *Immunol, 167*(10), 5749-5757. doi:10.4049/jimmunol.167.10.5749

448   Ma, Z., & Finkel, T. H. (2010). T cell receptor triggering by force. *Trends in immunology, 31*(1),
449   1-6. doi:10.1016/j.it.2009.09.008

450   Macián, F., García-Cózar, F., Im, S. H., Horton, H. F., Byrne, M. C., & Rao, A. (2002).
451   Transcriptional mechanisms underlying lymphocyte tolerance. *Cell, 109*(6), 719-731.
452   doi:10.1016/s0092-8674(02)00767-5

453 McCaffrey, P. G., Luo, C., Kerppola, T. K., Jain, J., Badalian, T. M., Ho, A. M., . . . et al. (1993).
454   Isolation of the cyclosporin-sensitive T cell transcription factor NFATp. *Science,*
455   *262*(5134), 750-754. doi:10.1126/science.8235597
456 Nicoli, F., Papagno, L., Frere, J. J., Cabral-Piccin, M. P., Clave, E., Gostick, E., . . . Appay, V.
457   (2018). Naïve CD8+ T-Cells Engage a Versatile Metabolic Program Upon Activation in
458   Humans and Differ Energetically From Memory CD8+ T-Cells. *9*(2736).
459   doi:10.3389/fimmu.2018.02736
460 Northrop, J. P., Ho, S. N., Chen, L., Thomas, D. J., Timmerman, L. A., Nolan, G. P., . . .
461   Crabtree, G. R. (1994). NF-AT components define a family of transcription factors
462   targeted in T-cell activation. *Nature, 369*(6480), 497-502. doi:10.1038/369497a0
463 Palazon, A., Goldrath, A. W., Nizet, V., & Johnson, R. S. (2014). HIF transcription factors,
464   inflammation, and immunity. *Immunity, 41*(4), 518-528.
465   doi:10.1016/j.immuni.2014.09.008
466 Piroth, L., Cottenet, J., Mariet, A. S., Bonniaud, P., Blot, M., Tubert-Bitter, P., & Quantin, C.
467   (2021). Comparison of the characteristics, morbidity, and mortality of COVID-19 and
468   seasonal influenza: a nationwide, population-based retrospective cohort study. *Lancet*
469   *Respir Med, 9*(3), 251-259. doi:10.1016/s2213-2600(20)30527-0
470 Ranade, S. S., Qiu, Z., Woo, S.-H., Hur, S. S., Murthy, S. E., Cahalan, S. M., . . . Patapoutian, A.
471   (2014). Piezo1, a mechanically activated ion channel, is required for vascular
472   development in mice. *111*(28), 10347-10352. doi:10.1073/pnas.1409233111 %J
473   Proceedings of the National Academy of Sciences
474 Robinson, M. D., McCarthy, D. J., & Smyth, G. K. (2010). edgeR: a Bioconductor package for
475   differential expression analysis of digital gene expression data. *Bioinformatics, 26*(1),
476   139-140. doi:10.1093/bioinformatics/btp616
477 Sadoshima, J., & Izumo, S. (1997). The cellular and molecular response of cardiac myocytes to
478   mechanical stress. *Annu Rev Physiol, 59*, 551-571. doi:10.1146/annurev.physiol.59.1.551
479 Schoen, K., Horvat, N., Guerreiro, N. F. C., de Castro, I., & de Giassi, K. S. (2019). Spectrum of
480   clinical and radiographic findings in patients with diagnosis of H1N1 and correlation with
481   clinical severity. *BMC Infect Dis, 19*(1), 964. doi:10.1186/s12879-019-4592-0
482 Solis, A. G., Bielecki, P., Steach, H. R., Sharma, L., Harman, C. C. D., Yun, S., . . . Flavell, R.
483   A. (2019). Mechanosensation of cyclical force by PIEZO1 is essential for innate
484   immunity. *Nature, 573*(7772), 69-74. doi:10.1038/s41586-019-1485-8
485 Takemoto, K., Ishihara, S., Mizutani, T., Kawabata, K., & Haga, H. (2015). Compressive stress
486   induces dephosphorylation of the myosin regulatory light chain via RhoA
487   phosphorylation by the adenylyl cyclase/protein kinase A signaling pathway. *PloS one,*
488   *10*(3), e0117937. doi:10.1371/journal.pone.0117937
489 Teramura, T., Takehara, T., Onodera, Y., Nakagawa, K., Hamanishi, C., & Fukuda, K. (2012).
490   Mechanical stimulation of cyclic tensile strain induces reduction of pluripotent related
491   gene expressions via activation of Rho/ROCK and subsequent decreasing of AKT
492   phosphorylation in human induced pluripotent stem cells. *Biochem Biophys Res*
493   *Commun, 417*(2), 836-841. doi:10.1016/j.bbrc.2011.12.052
494 Tharaux, P. L., Bukoski, R. C., Rocha, P. N., Crowley, S. D., Ruiz, P., Nataraj, C., . . . Coffman,
495   T. M. (2003). Rho kinase promotes alloimmune responses by regulating the proliferation
496   and structure of T cells. *J Immunol, 171*(1), 96-105. doi:10.4049/jimmunol.171.1.96
497 Wahl, A., Dinet, C., Dillard, P., Nassereddine, A., Puech, P. H., Limozin, L., & Sengupta, K.
498   (2019). Biphasic mechanosensitivity of T cell receptor-mediated spreading of

499   lymphocytes. *Proc Natl Acad Sci U S A, 116*(13), 5908-5913.
500   doi:10.1073/pnas.1811516116
501 Walczak-Drzewiecka, A., Ratajewski, M., Wagner, W., & Dastych, J. (2008). HIF-1alpha is up-
502   regulated in activated mast cells by a process that involves calcineurin and NFAT. *J*
503   *Immunol, 181*(3), 1665-1672. doi:10.4049/jimmunol.181.3.1665
504 Wang, R., Dillon, C. P., Shi, L. Z., Milasta, S., Carter, R., Finkelstein, D., . . . Green, D. R.
505   (2011). The transcription factor Myc controls metabolic reprogramming upon T
506   lymphocyte activation. *Immunity, 35*(6), 871-882. doi:10.1016/j.immuni.2011.09.021
507 Wu, C., Orozco, C., Boyer, J., Leglise, M., Goodale, J., Batalov, S., . . . Su, A. I. (2009).
508   BioGPS: an extensible and customizable portal for querying and organizing gene
509   annotation resources. *Genome Biol, 10*(11), R130. doi:10.1186/gb-2009-10-11-r130
510 Zheng, H. Y., Xu, M., Yang, C. X., Tian, R. R., Zhang, M., Li, J. J., . . . Zheng, Y. T. (2020).
511   Longitudinal transcriptome analyses show robust T cell immunity during recovery from
512   COVID-19. *Signal Transduct Target Ther, 5*(1), 294. doi:10.1038/s41392-020-00457-4

513

Figures legends

Fig. 1. The expression of the activation marker CD69 and cytokines in lymphocytes following mechanical stressing. (A) Flow cytometry analysis on CD69 expression among CD4+, CD8+, and CD19+ cells following LPS, or PMA/I stimulation compared to resting lymphocytes. Pseudocolored plots indicating mechanical stressing effect, and data represent the results of 4 independent experiments. **(B)** Bar graphs indicating mechanical stressing effect on mRNA fold changes of *Tnf, Ifng*, *Il1b*, *Il2*, *Il4*, *Il10* in lymphocytes following LPS, or PMA/I stimulation compared to resting lymphocytes (Data represent the results of 4 independent experiments, mRNA fold changes are calculated to the Control $2^{-\Delta C'T}$). **(C)** Bar graphs indicating mechanical stressing effect on IL-2, IFN-γ, and TNF-a levels as evaluated by ELISA assay in culture medium of PMA/I-stimulated lymphocytes compared to resting lymphocytes (Figures represent the results of 6 independent experiments, data are represented as mean ± SD); (Mechanical stressing: 50 mmHg/3 hr); Abbreviations: LPS= Lipopolysaccharide, PMA/I= Phorbol myristate acetate/Ionomycin, MFI= Median Fluorescence Intensity, mmHg= millimeter of mercury, ***** P ≤ 0.05, ****** P ≤ 0.01, ******* P ≤ 0.001.

Fig. 2. The expression of the activation marker CD69 and cytokines in lymphocytes following PIEZO1 activation using Yoda1. (A) Flow cytometry analysis on CD69 expression among CD4+, CD8+, and CD19+ cells following PMA/I and Yoda1 treatments. **(B)** Bar graphs indicating Yoda1 effect on IL-2, IFN-γ, and TNF-a levels as evaluated by ELISA assay in culture medium of PMA/I-stimulated lymphocytes compared to resting lymphocytes. (Data represent the results of 3 independent experiments, data are represented as mean ± SD); (Yoda1: 10 μM/3 hr); Abbreviations: MFI= Median Fluorescence Intensity, O.D= optical Density, PMA/I= Phorbol myristate acetate/Ionomycin, * P ≤ 0.05, ** P ≤ 0.01.

Fig. 3. NFAT1 expression changes in lymphocytes following mechanical stressing. (A) NFAT1 expression changes in CD4+ cells following PMA/I stimulation and mechanical stressing (Yellow= NFAT1, Cyan= DAPI, Green= CD4). **(B)** Bar graphs indicating the nuclear, cytoplasmic, and total relative expression changes of NFAT1 in CD4+ cells. **(C)** NFAT1 expression changes in CD8+ cells following PMA/I stimulation and mechanical stressing (Yellow= NFAT1, Cyan= DAPI, Red= CD8). **(D)** Bar graphs indicating the relative expression of NFAT1 in CD8+ cells in nucleus, cytoplasm, and total cell. (Mechanical stressing: 50 mmHg/3 hr). (Data represent the results of 3 independent experiments, data are represented as mean ± SD); Abbreviations: MFI= Mean Fluorescence Intensity, mmHg= millimeter of mercury, PMA/I= Phorbol myristate acetate/Ionomycin. ** P ≤ 0.05, ** P ≤ 0.01.

Fig. 4. *Jun* and *Fos* mRNA expression changes following mechanical stressing in lymphocytes. Bar graphs indicating mechanical stressing effect on mRNA expression changes of *Jun* and *Fos* in PMA/I-stimulated lymphocytes compared to resting lymphocytes (Data represent the results of 4 independent experiments, mRNA fold changes are calculated to the Control $2^{-\Delta C'T}$, data are

551   represented as mean ± SD); (Mechanical stressing: 50 mmHg/3 hr); Abbreviations: PMA/I=

552   Phorbol myristate acetate/Ionomycin, mmHg= millimeter of mercury, ***** P ≤ 0.05.

553   **Fig. 5. Hypertension comorbidity effect on the expression of lymphocyte activation related**

554   **genes in peripheral blood mononuclear cells from COVID19 patients.** Bar graphs indicating

555   logFC changes for the expression of *JUN*, *FOS*, *CD69*, *IFNG*, and *TNF* when comparing

556   hypertensive COVID-19 patients [HT] to normotensive COVID-19 patients [NT] in both

557   treatment stage and rehabilitation stage. (Treatment stage comparison include 4 HT patients and

558   4 NT patients; Rehabilitation stage comparison include 2 HT patients and 3 NT patients);

559   log2FC= edgeR Log2 fold change. * P ≤ 0.05 (edgeR P value).

Fig. 1

Fig. 2

Fig. 3

Fig. 4

| PMA/I | − | − | + | + |
| 50 mmHg | − | + | − | + |

| PMA/I | − | − | + | + |
| 50 mmHg | − | + | − | + |

Fig. 5

Fig. S1

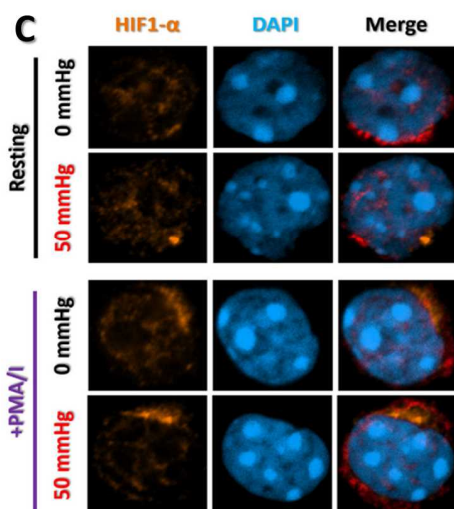Fig. S2

A

B
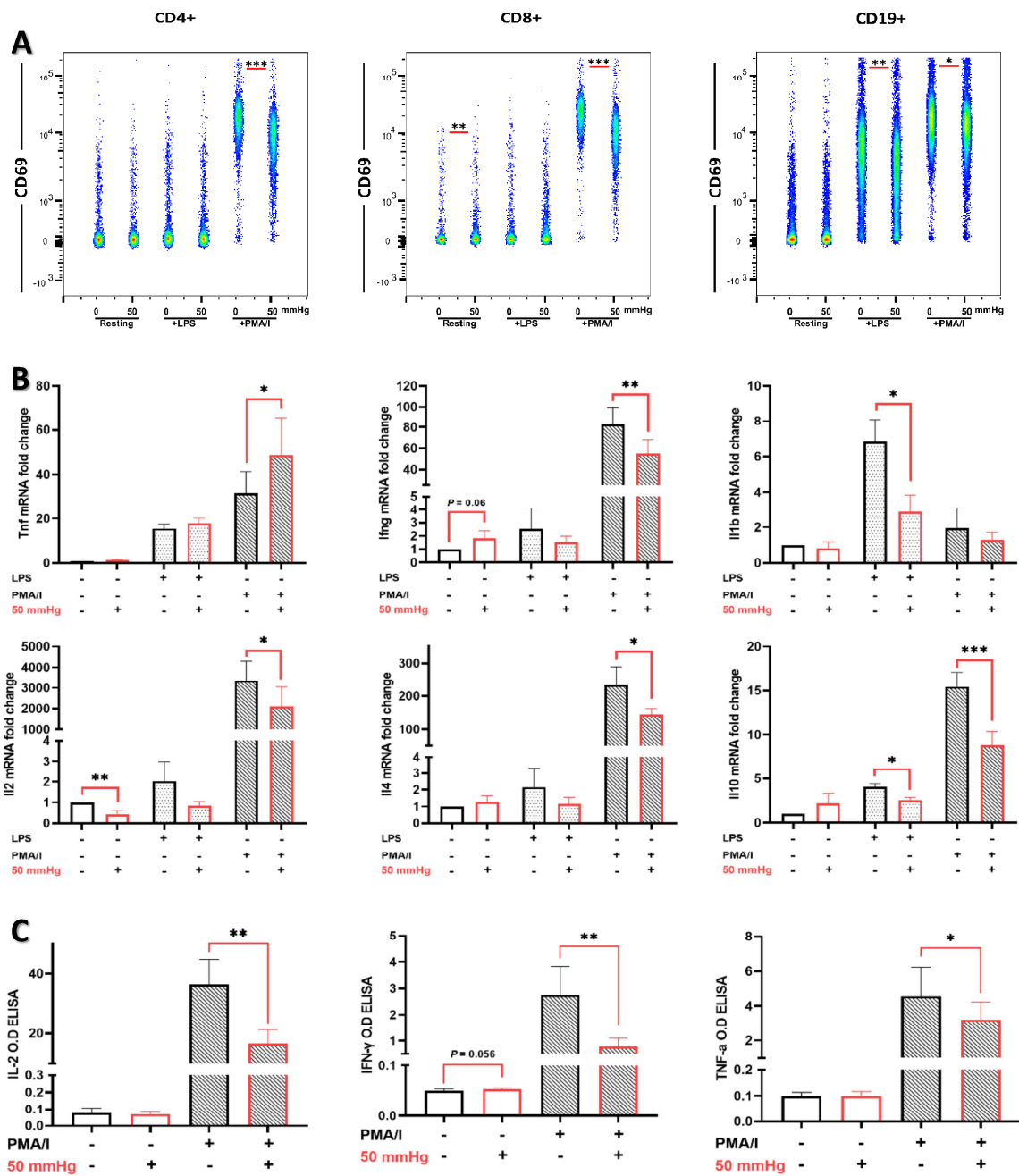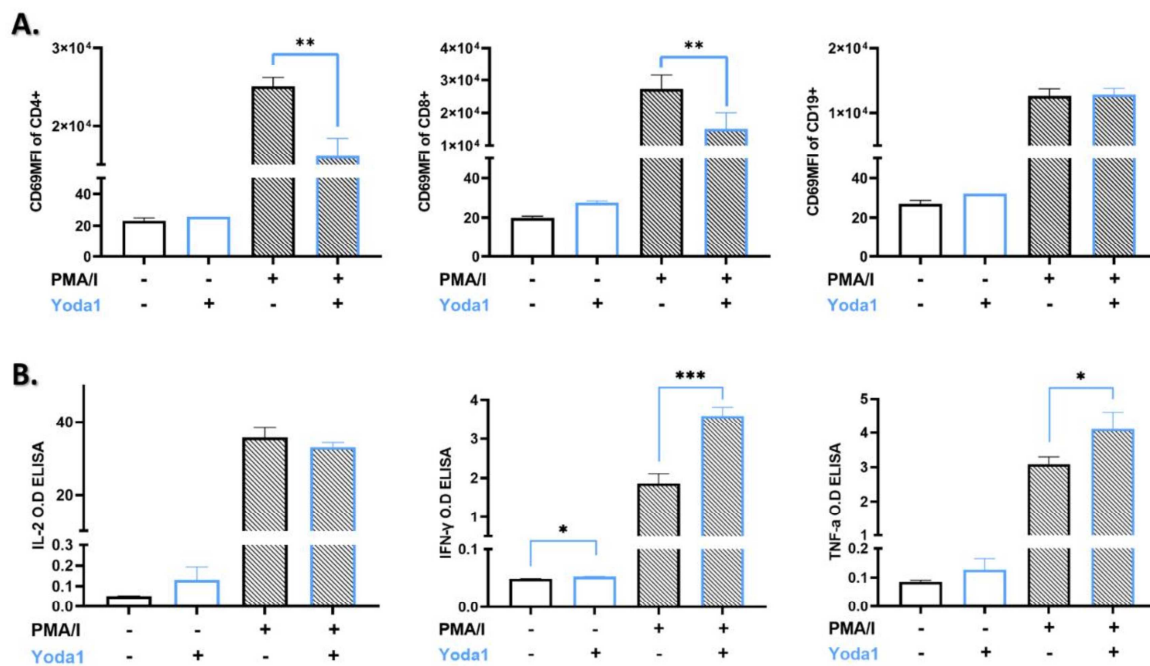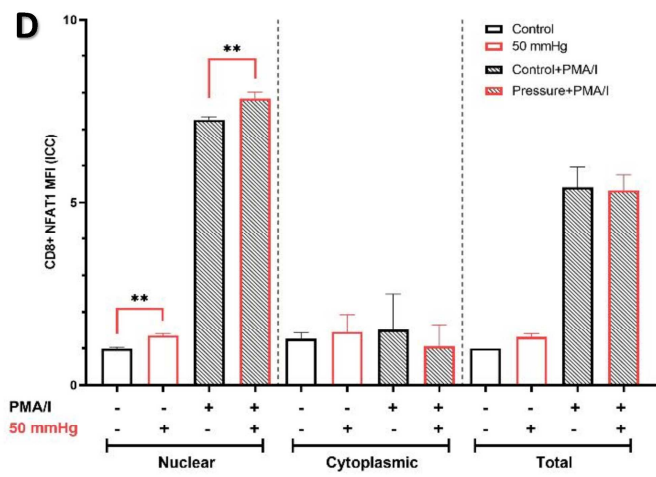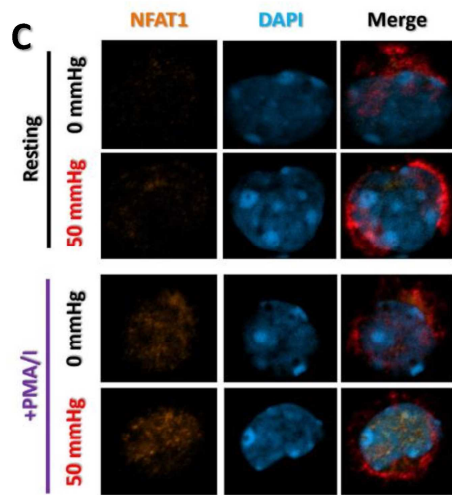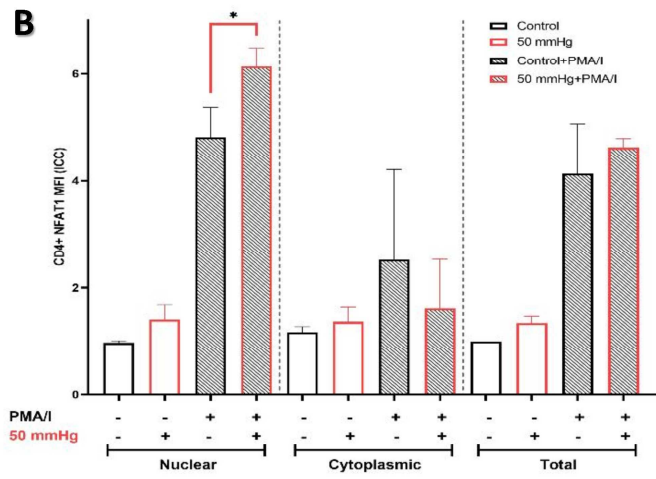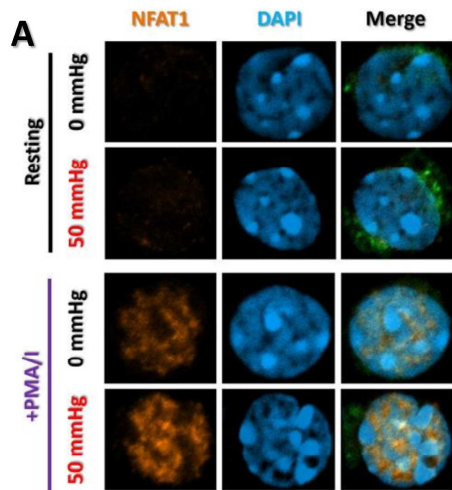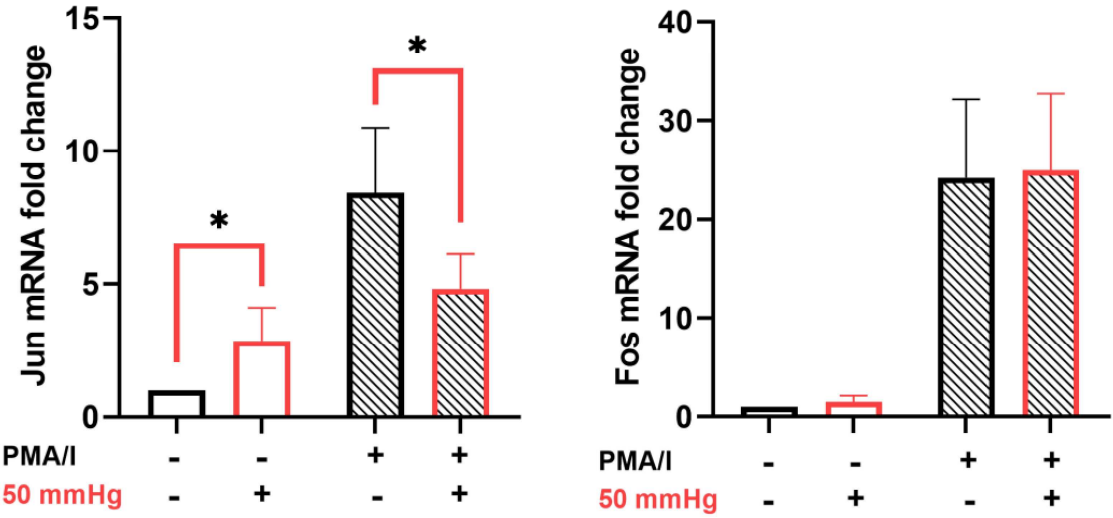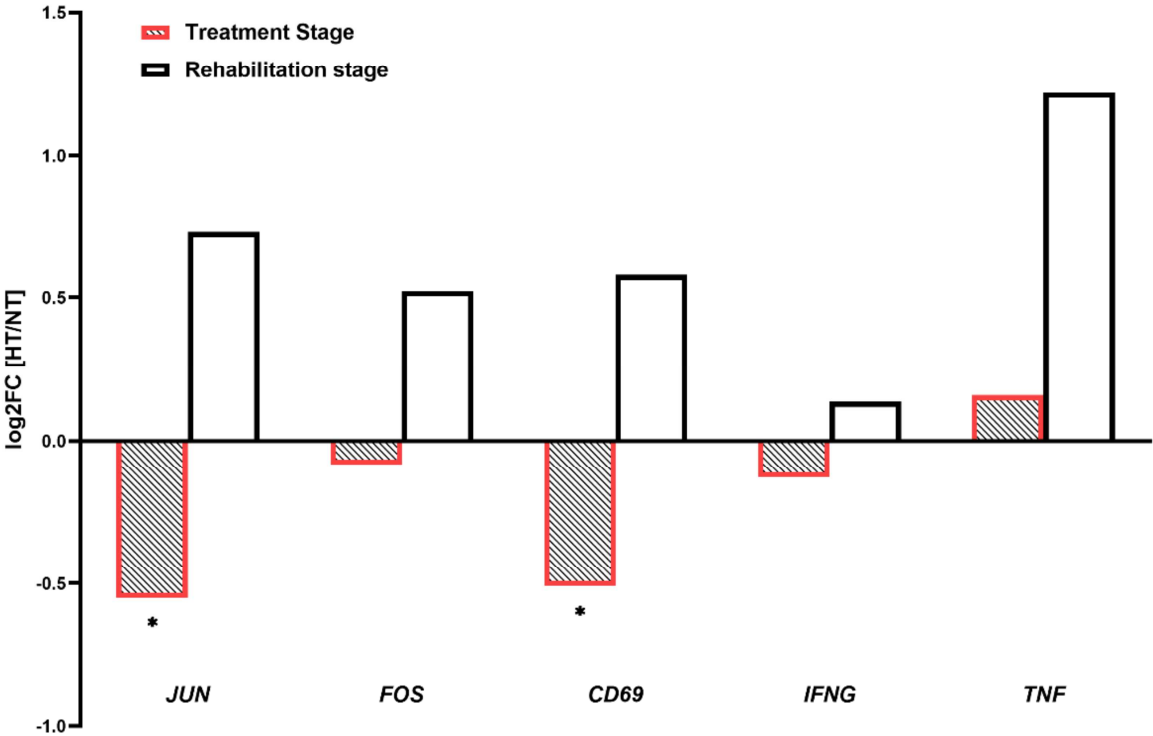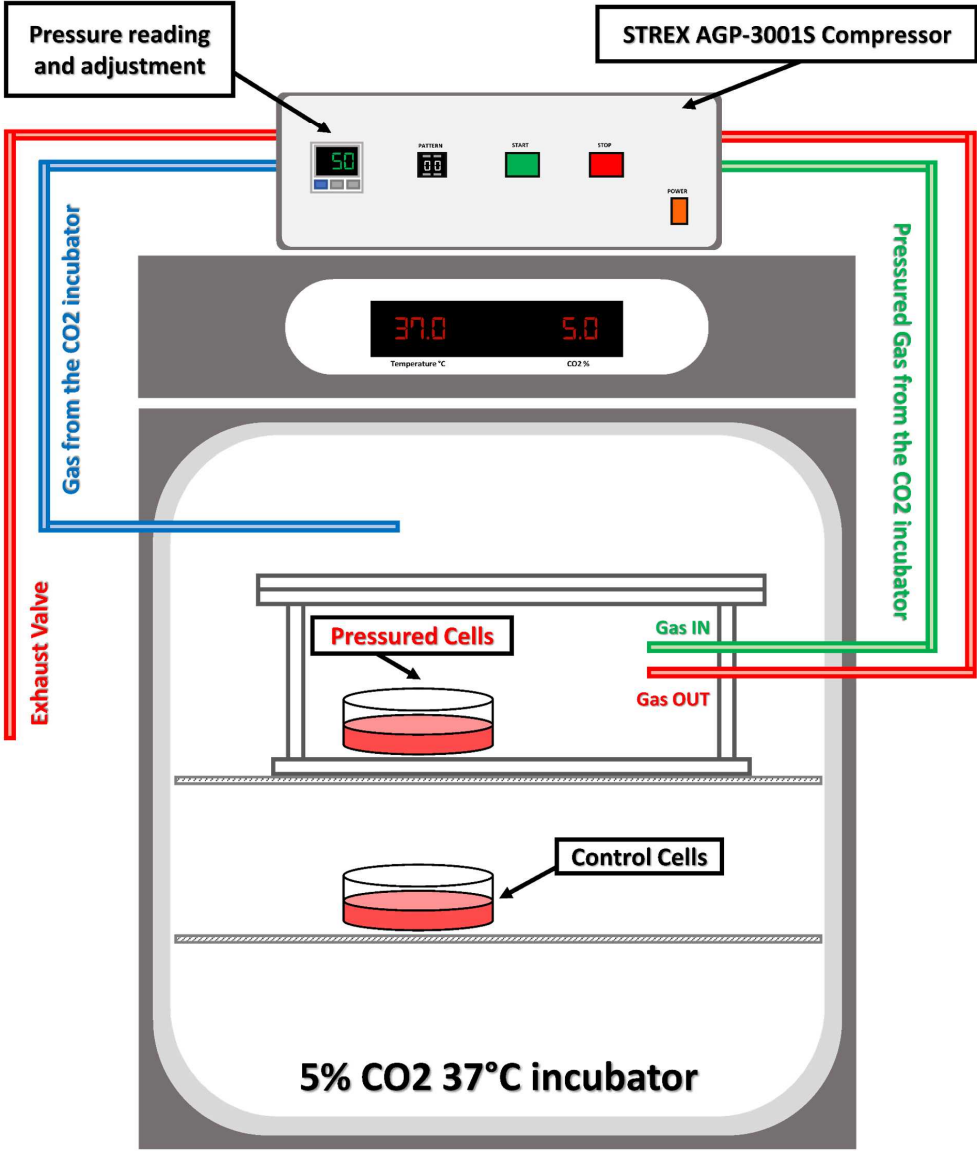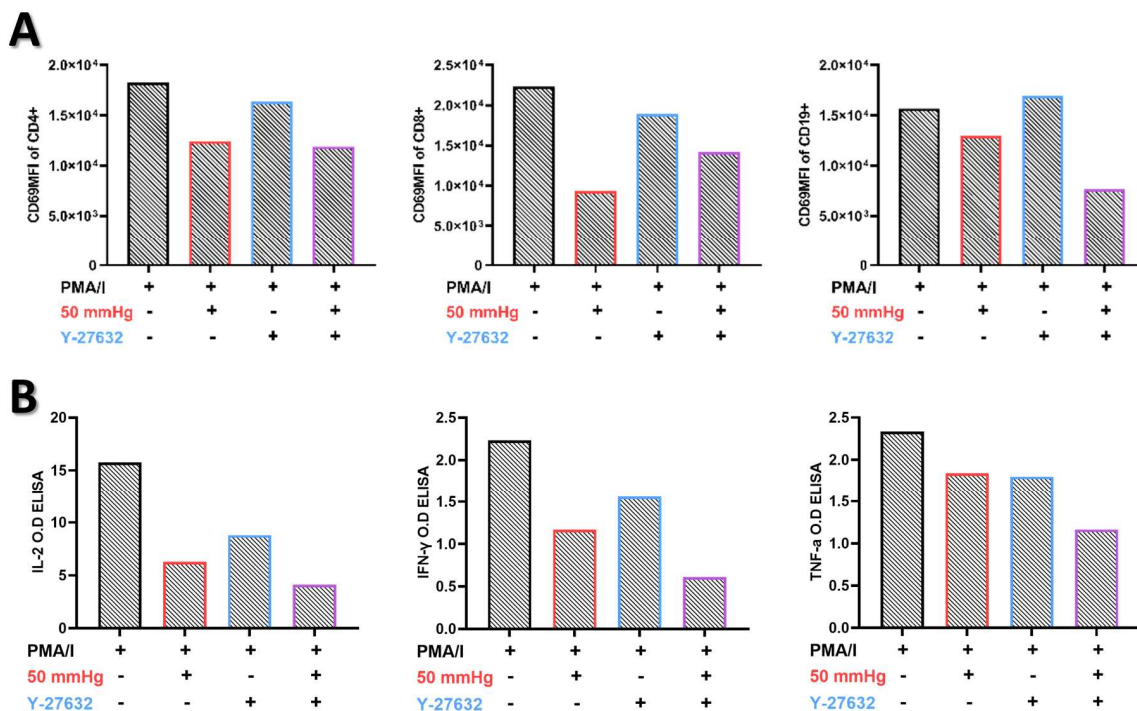
Fig. S3
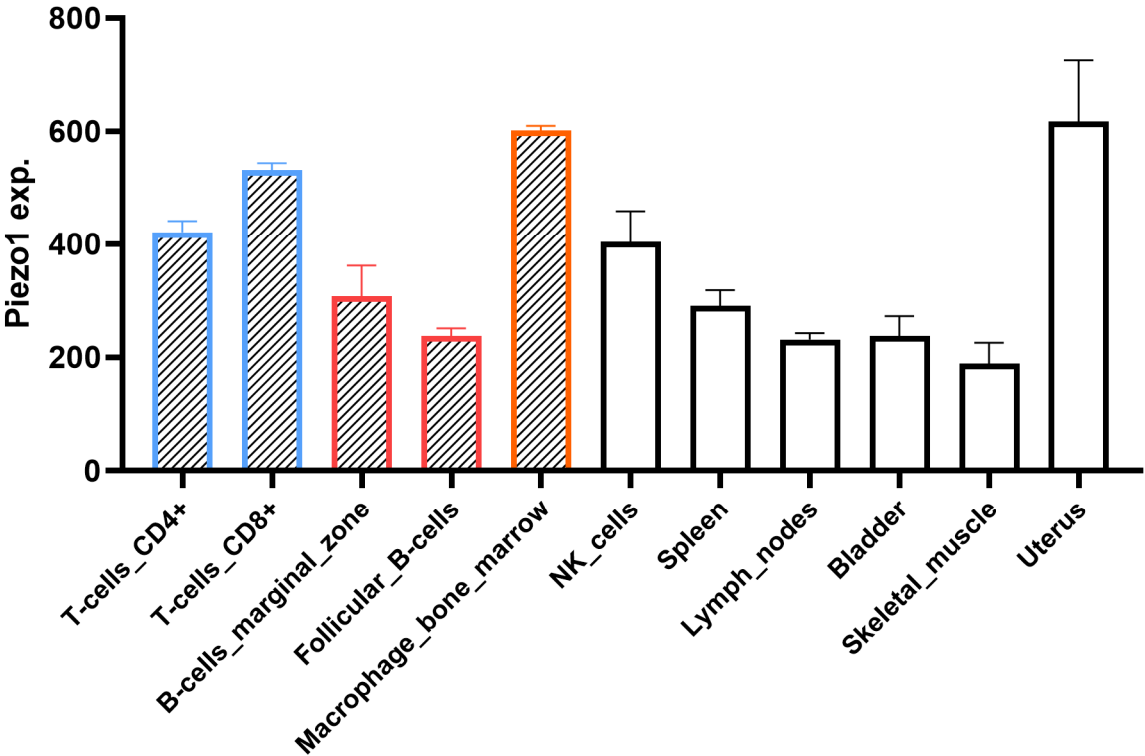
Fig. S4
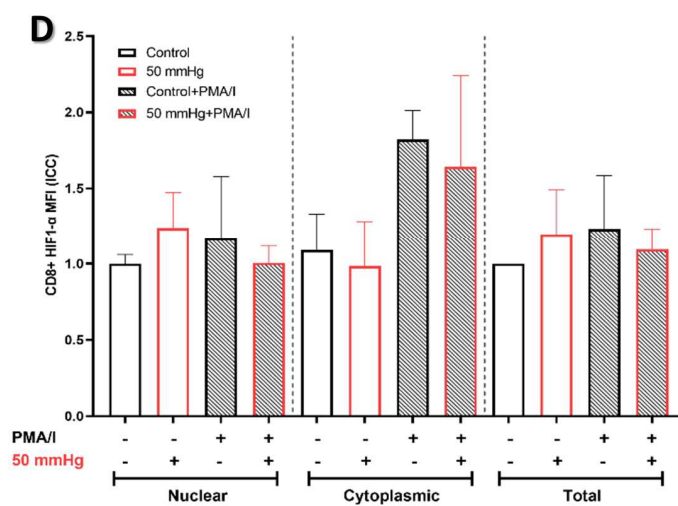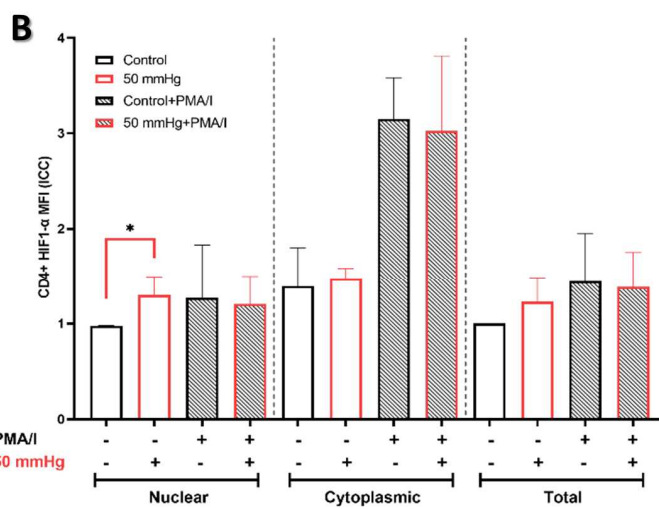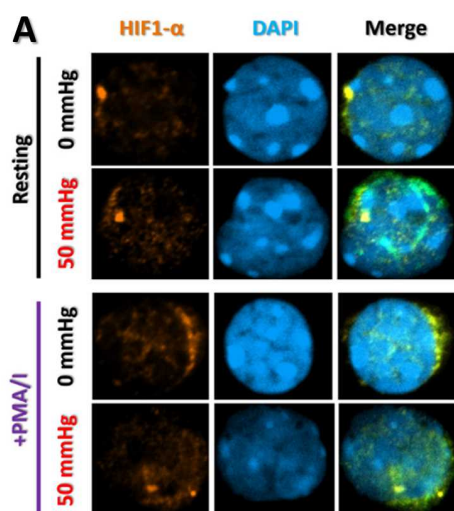
Fig. S5
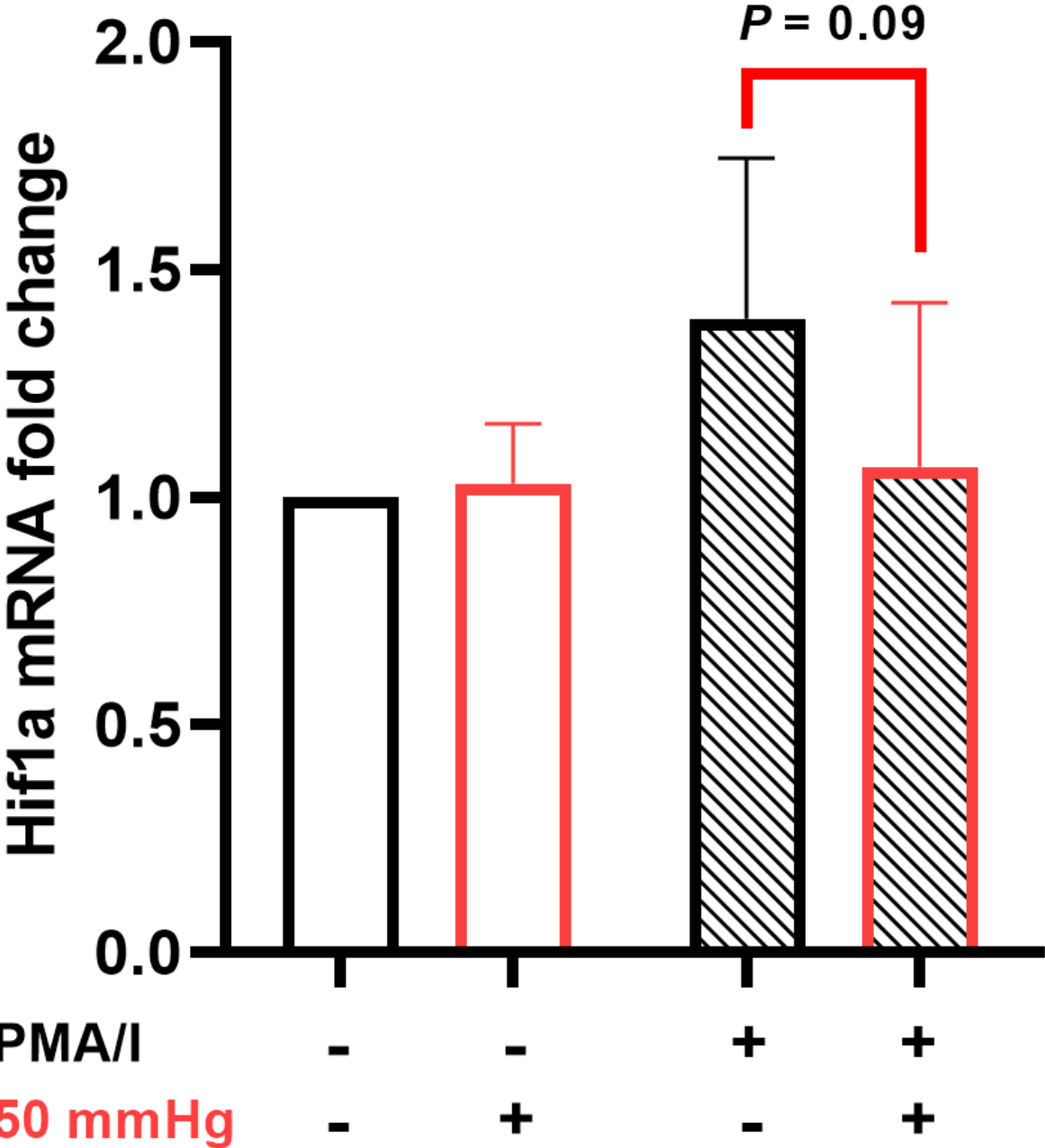
Table S1. List of Media, Chemicals.

Media, Buffers	Vendor	Catalog Number
RPMI-1640 with L-Glutamine	Wako	189-02025
HyClone FBS characterized	GE health Life Science	SH30071.03
Lipopolysaccharides E. coli O55:B5	Sigma	L2880-10MG
Yoda1, Piezo1 agonist	Cayman Chemical	21904
Y27632, ROCK inhibitor	ATCC	ACS3030
Cell Activation Cocktail (PMA/Ionomycin)	BioLegend	423302

Table S2. List of Antibodies.

Antibody, Probe	Vendor	Catalog Number	Dilution Flow	Dilution ICC
CD4-FITC	Invitrogen	11-0041-81	1:200	1:100
CD8a-APC	BioLegend	100711	1:120	1:100
CD19-APC	BioLegend	115511	1:120	-
CD69-PE	BioLegend	104508	1:120	-
HIF1-α	Novus Biologicals	NB100-134	-	1:120
NFAT1	Cell Signaling Technology	5861	-	1:120
Goat anti-Rabbit IgG (H+L) Alexa Fluor 546	Invitrogen	A-11035	-	1:1000
Goat anti-Rabbit IgG (H+L) Alexa Fluor Plus 647	Invitrogen	A32733	-	1:1000
DAPI (4′,6-diamidino-2-phenylindole)	Invitrogen	D21490	-	1:2000
Transcription Factor Staining Buffer Set	Invitrogen	00-5523-00		
Mouse FcR Blocking Reagent	Miltenyi Biotec	130-092-575	1:10	1:10

Table S3. List of Primers.

Target	Fwd Primer Sequence	Rev Primer Sequence
Actb	GTACCACCATGTACCCAGGC	AACGCAGCTCAGTAACAGTCC
Fos	TCCCCAAACTTCGACCATG	GCACTAGAGACGGACAGATC
Hif1a	ACCTTCATCGGAAACTCCAAAG	CTGTTAGGCTGGGAAAAGTTAGG
Ifng	TCAAGTGGCATAGATGTGGAAGA	TGGCTCTGCAGGATTTTCATG
Il10	GCTCTTACTGACTGGCATGAG	CGCAGCTCTAGGAGCATGTG
Il1b	GCAACTGTTCCTGAACTCAACT	ATCTTTTGGGGTCCGTCAACT
Il2	TGAGCAGGATGGAGAATTACAGG	GTCCAAGTTCATCTTCTAGGCAC
Il4	ATGGAGCTGCAGAGACTCTT	AAAGCATGGTGGCTCAGTAC
Jun	GCAGAAAGTCATGAACCACG	AGTCCATCTTGTGTACCCTTG
Tnf	CCAGACCCTCACACTCAGATC	CACTTGGTGGTTTGCTACGAC